Electronic Supplementary Material (ESI) for Journal of Materials Chemistry C.

Supporting information to

Simultaneous enhancement of charge generation quantum yield and carrier transport in organic solar cells

Ardalan Armin[1], Pascal Wolfer[1], Paul E. Shaw[1], Mike Hambsch[1], Fatemeh Maasoumi[1], Mujeeb Ullah[1], Eliot Gann[2], Christopher R. McNeill[2], Jun Li[3], Zugui Shi[3], Paul L, Burn[1*] and Paul Meredith[1]*

[1]Centre for Organic Photonics & Electronics (COPE), School of Mathematics and Physics and School of Chemistry and Molecular Biosciences, The University of Queensland, Brisbane 4072, Australia, [2]Department of Materials Engineering, Monash University, Clayton, Victoria 3800, Australia, [3]Institute of Materials Research and Engineering, Agency for Science, Technology and Research, Singapore 117602

KEYWORDS: bulk heterojunction, nanostructure, charge carrier transport, organic solar cell, charge generation

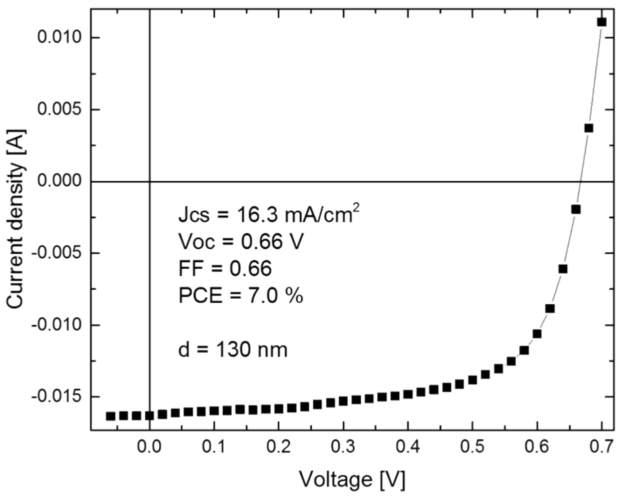

Figure S1. *J-V* curve of the "hero" DPP-DTT:PC70BM device delivering 7% power conversion efficiency.

MIS-CELIV: In the following, we briefly explain the working principles of the technique. MIS-CELIV uses a metal-insulator-semiconductor architecture where MgF_2 is the insulator (dielectric) layer. To perform the experiment, as shown in **Figure S2 (a)**, an initial offset voltage is applied to the device ($t < 0$), which injects one type of carrier (holes or electrons depending on the polarity and the position of the insulator layer). To be able to inject charge carriers, the work function of the injecting electrode is of importance. For the hole-only devices the architecture was ITO/MgF2/semiconductor/MoOx/Ag and for the electron-only devices ITO/MgF2/semiconductor/Al. The offset voltage is such that the potential is positive on the MoOx/Ag electrode for the former to inject holes, and negative on Al for the later to inject electrons. At sufficiently large offset voltage ($V_{\text{off}} >> KT/e$) a thin sheet of charges is formed at the interface with the insulator. A triangle voltage pulse in the opposite direction of the offset polarity is then applied to extract the injected charges, which are accumulated at the interface. In this case the current initially reaches a displacement level (j_0), which corresponds to the capacitance of the whole diode [**Figure S2 (b)**]. Then the current increases until reaching a peak when the charge carriers reach the electrode (transit time). In the case of applying a large voltage offset, the amount of injected carriers is large enough so that at the start of the extraction, the current increases to a secondary displacement level with a quadratic behaviour versus time as a result of forming space charges within the semiconductor where the electric field is screened. The secondary displacement current corresponds to the capacitance level of the dielectric layer, which is chosen to be larger than the capacitance of the whole diode. The transit time of the carriers can then be measured very precisely as the time it takes until the current reaches $2J_0$. From the transit time it is possible to calculate the mobility of the relevant carrier.

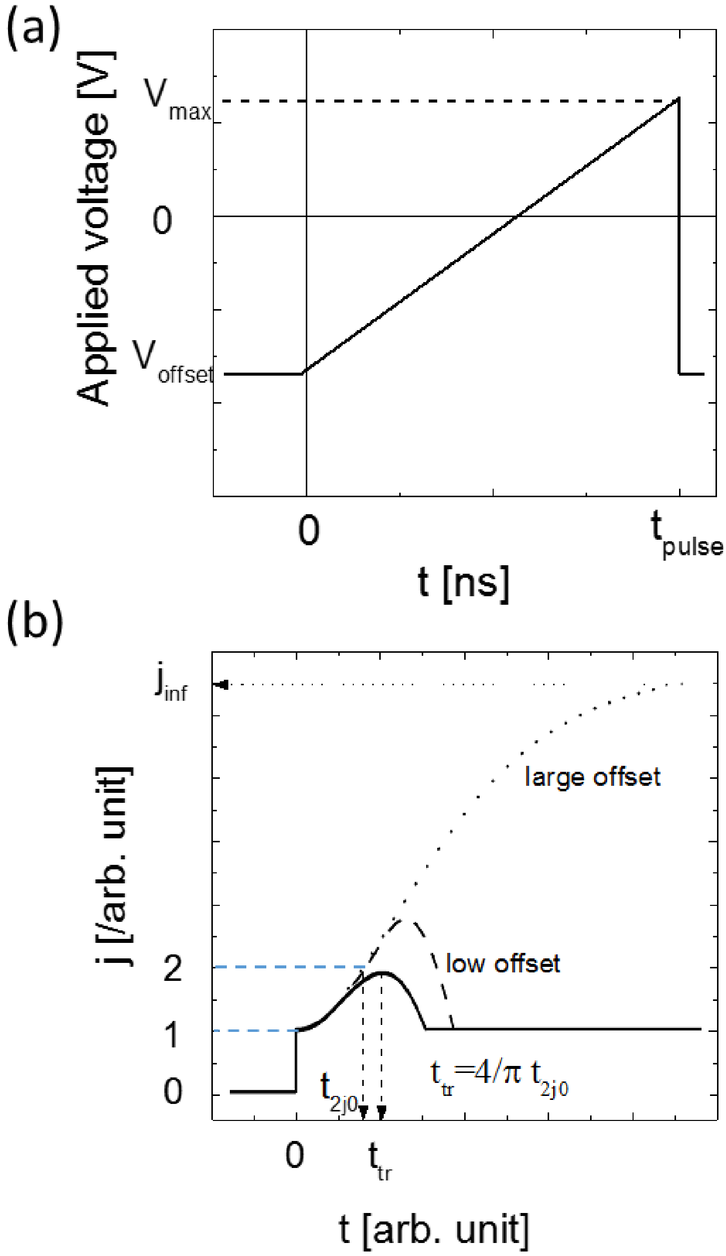

Figure S2. (a) Applied CELIV voltage pulse to perform MIS-CELIV. An initial voltage offset is applied initially in forward bias direction to inject the carriers (holes or electrons) and the triangle voltage extracts the injected carriers, which can be accumulated near the interface of semiconductor/ dielectric layer (b) schematic MIS-CELIV current transients for different offset voltages. In the case of a small offset the extraction peak is the charge carrier transit time. For larger offset voltages space charges form during the extraction and the carrier transit time can be calculated from t_{2j0} as shown in the figure.

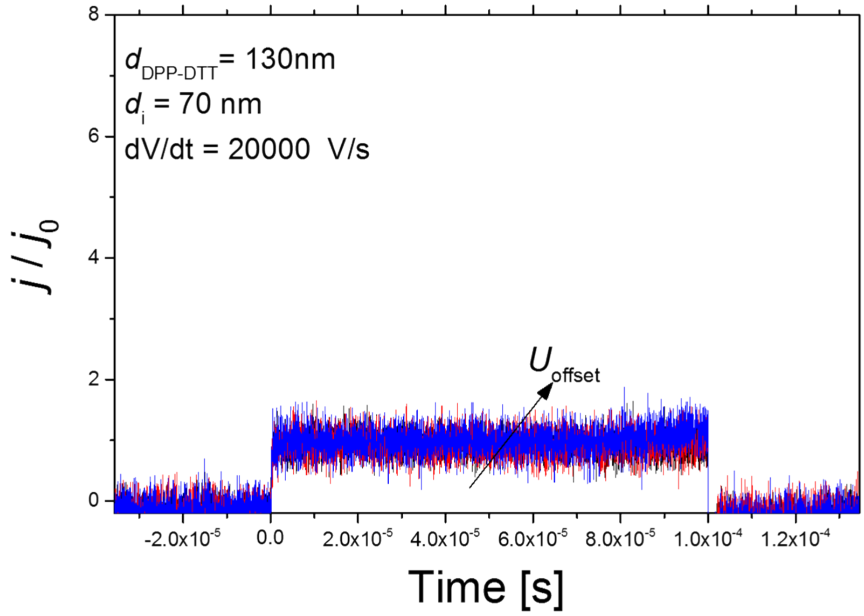

Figure S3. MIS-CELIV current transients of CF-DCB-cast DPP-DTT at different negative offset voltages (at t < 0). The absence of extraction current at t > 0 indicates the absence of mobile electrons and the electron mobility in this system is ~0.

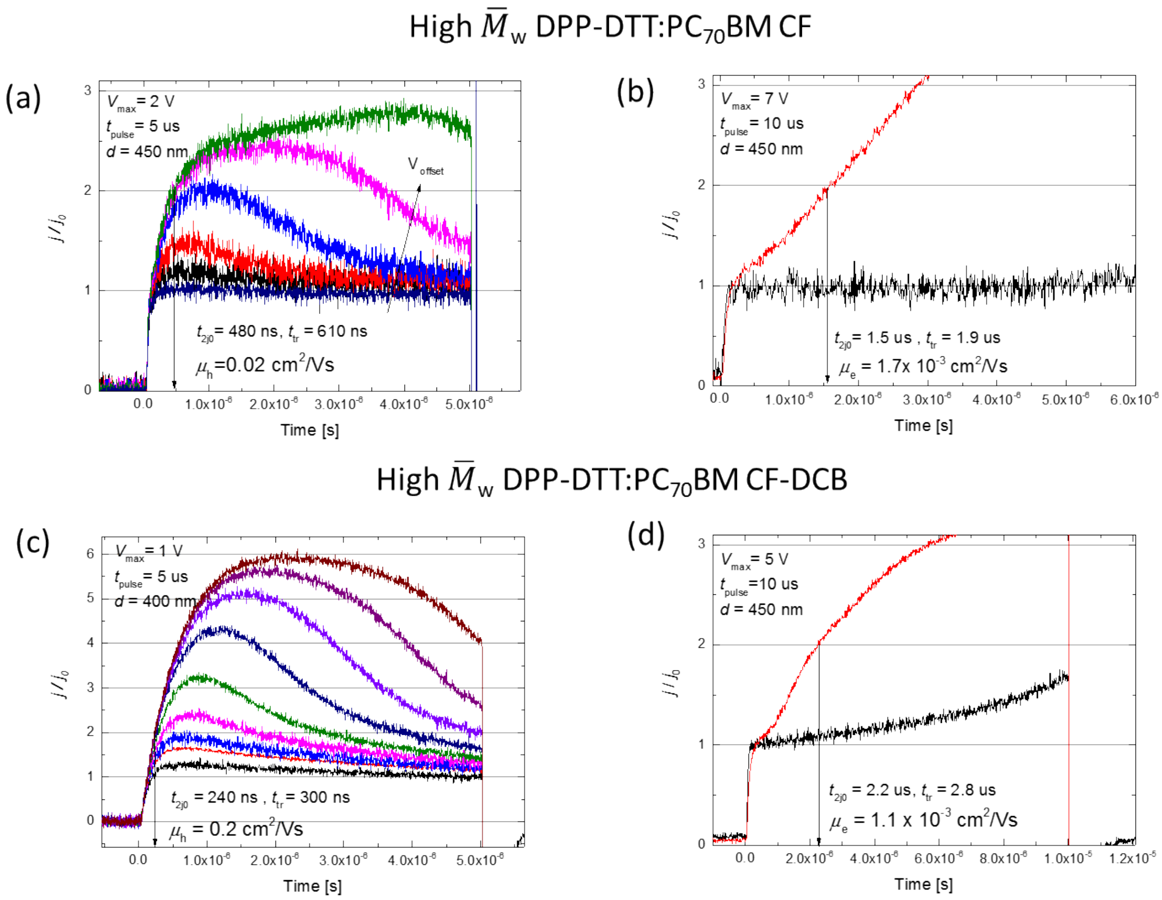

Figure S4. MIS-CELIV transients for a high $\overline{M}_w$ DPP-DTT:PC70BM blend film cast from CF and CF-DCB. (a) and (b) hole and electron transport in a CF-cast blend film, (c) and (d) hole and electron transport in a CF-DCB-cast blend film. The insulator was 70 nm thick MgF_2.

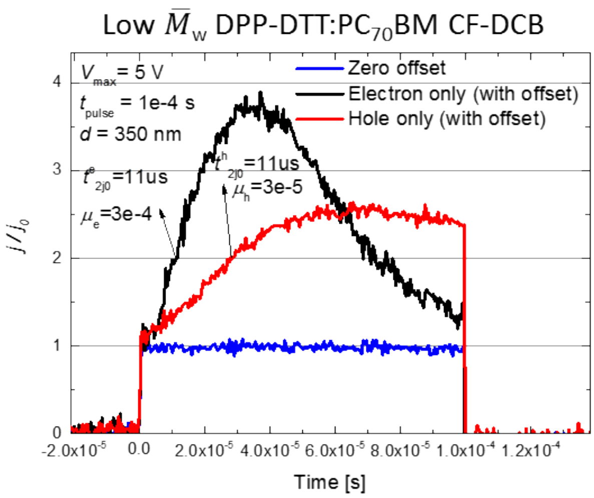

Figure S5. MIS-CELIV transients for a low $\overline{M}_w$ DPP-DTT:PC70BM blend film cast from CF-DCB.

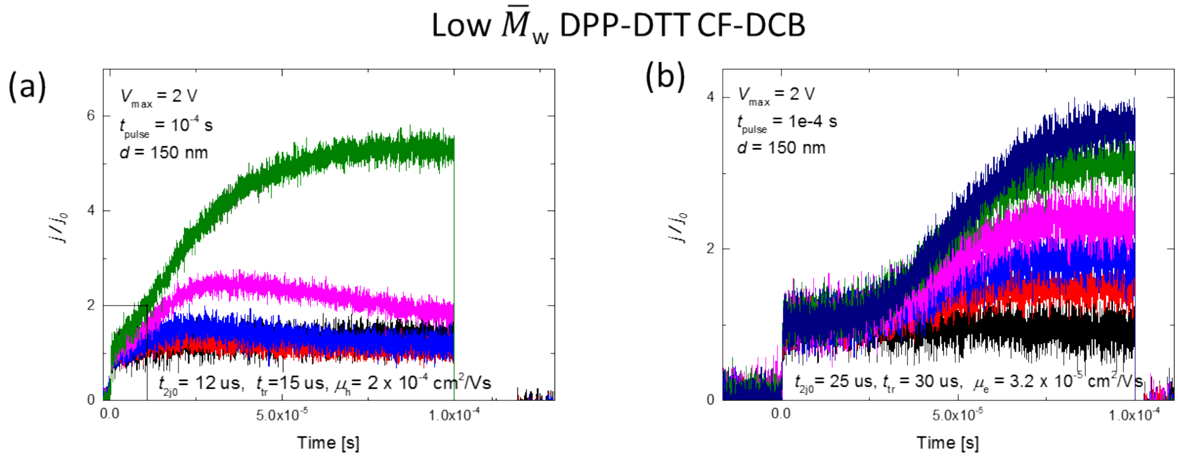

Figure S6. MIS-CELIV transients for a low $\bar{M}_w$ DPP-DTT:PC70BM blend film cast from CF-DCB. (a) hole transport and (b) electron transport. The insulator was 70 nm thick MgF_2.

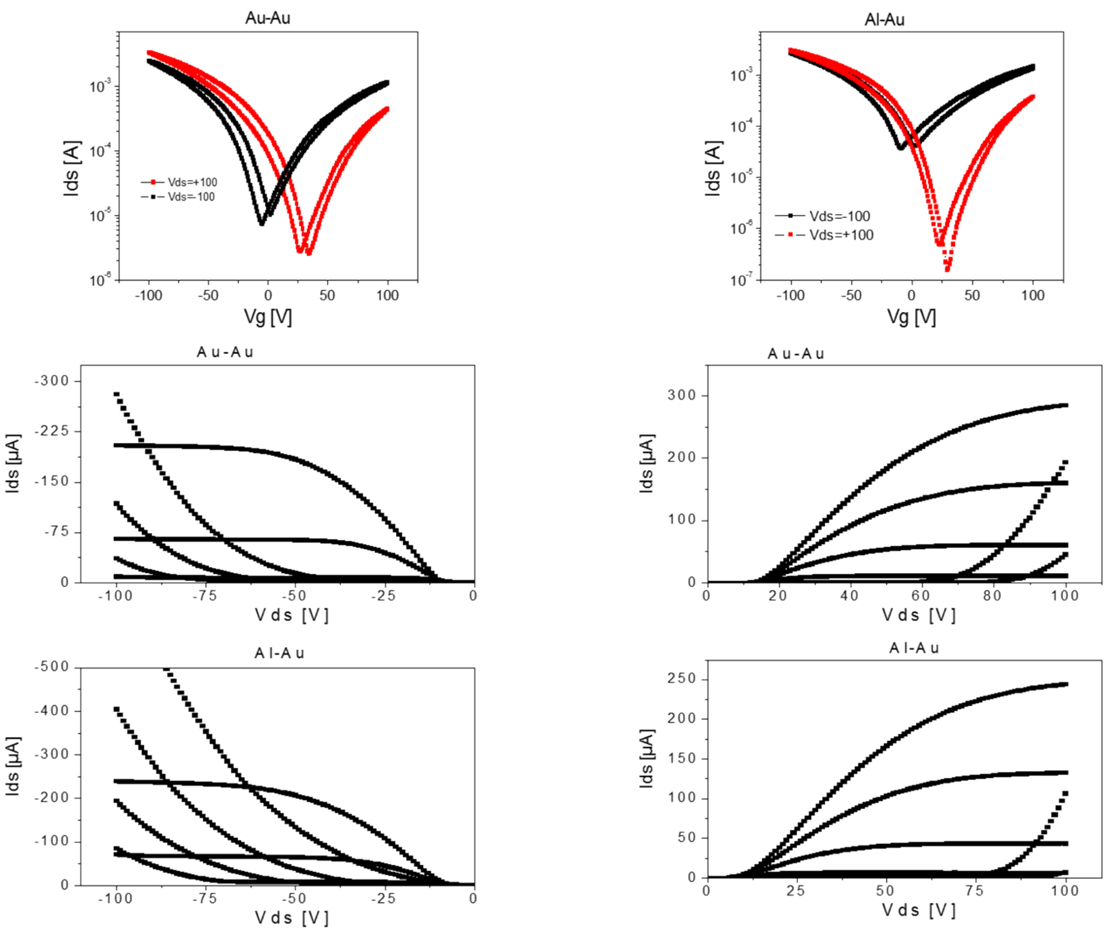

Figure S7. Transfer and output characteristics of high $\bar{M}_w$ DPP-DTT (CF-DCB casted) field effect transistors (FET) for both p- and n-channel.

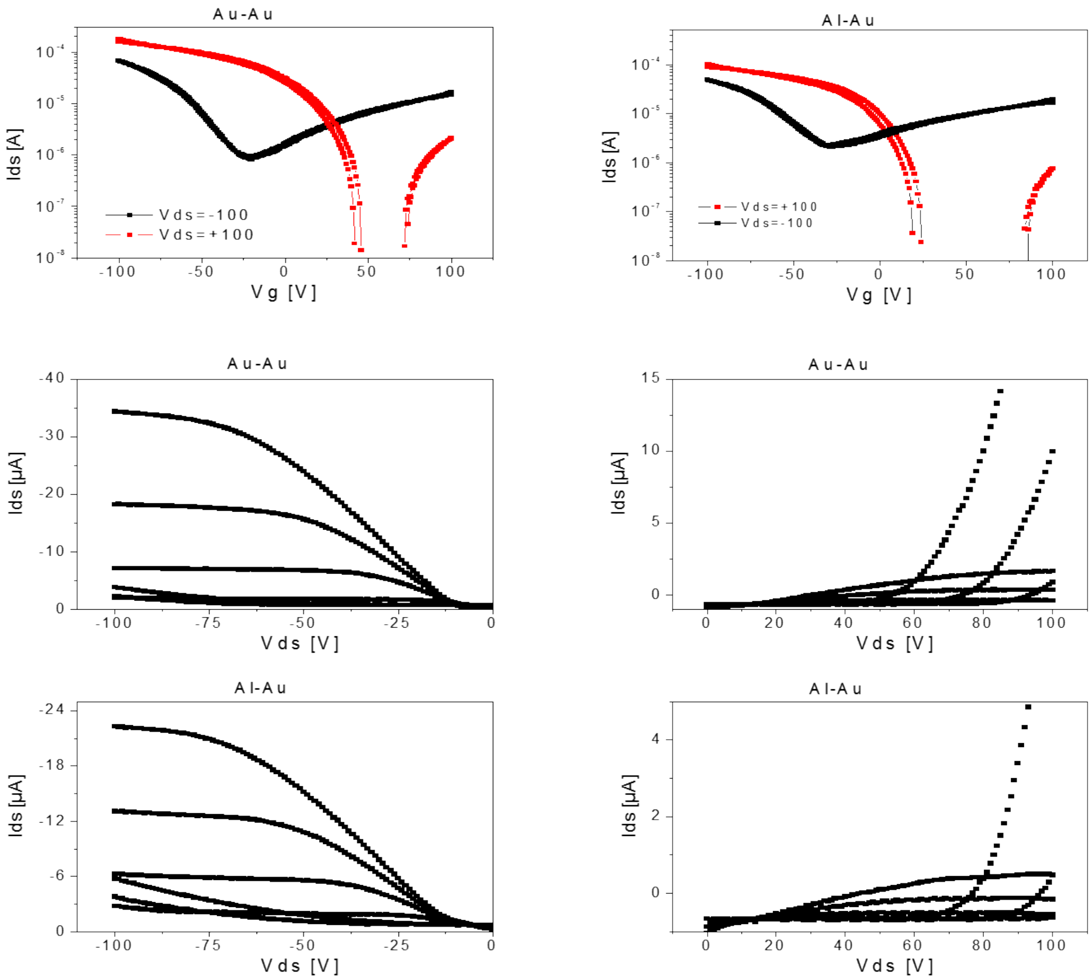

Figure S8. Transfer and output characteristics of low $\bar{M}_w$ DPP-DTT (CF-DCB casted) field effect transistors (FET) for both p- and n-channel.

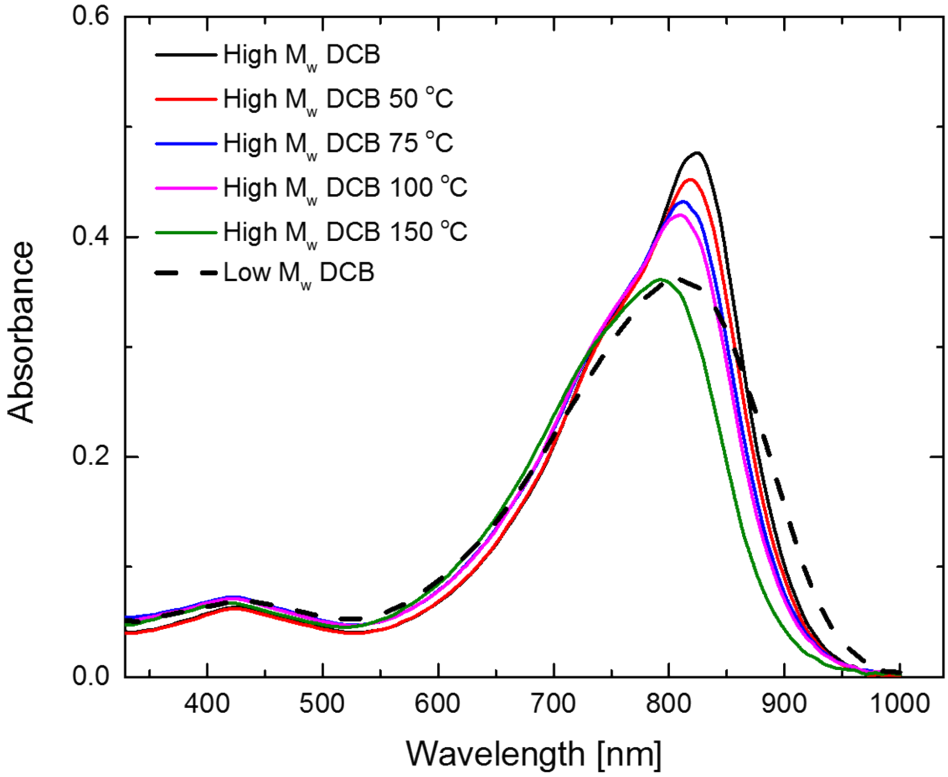

Figure S9. Solution absorption of high $\bar{M}_{\mathrm{w}}$ DPP-DTT in DCB at different temperatures compared with low $\bar{M}_{\mathrm{w}}$ also in DCB. The absorption shoulder near 800 nm disappears with increasing temperature due to weaker intermolecular interactions in a similar manner to the low $\bar{M}_{\mathrm{w}}$ polymer.